Journal of Engineering Physics and Thermophysics, Vol. 79, No. 3, 2006

NUMERICAL SIMULATION OF A VISCOUS SEPARATION FLOW AROUND A ROTATING CIRCULAR CYLINDER

A. B. Mazo and I. V. Morenko

UDC 532.516

Results of numerical solution of Navier–Stokes equations in stream function–vortex variables for a nonstationary laminar flow around a circular cylinder with a rotational degree of freedom are presented. The cases of definite, free, and inertial rotation of the indicated cylinder were considered.

The problem on a plane laminar flow of an incompressible viscous fluid around a circular cylinder is a classical model problem of hydrodynamics. The theoretical interest shown in this problem is explained, first of all, by the fact that an increase in the velocity of an incident flow (Reynolds number) causes a flow around a circular cylinder to change radically — the regime of flow without separation gives way to a self-oscillation regime, where the flow periodically separates from the surface of the cylinder and a Kármán vortex street is formed downstream of it [1–3]. Such a change in the regime of a flow, arising when a cylinder is instantaneously introduced into it, can also happen in the case of fairly large constant Re numbers.

In the majority of works on numerical simulation of this class of flows, a cylinder was assumed to be immovable [1, 3]. However, considerable recent attention has been focused on the more general problems concerning the interaction of a laminar flow with bodies around which it flows [4–8]. For example, in [5–8], the influence of a regular rotation of a cylinder on the character of vortices formed in a flow around it was investigated.

The present work is devoted to numerical investigation of the general problem on a nonstationary separation flow around a circular cylinder with a rotational degree of freedom. The interaction of the flow with the cylinder in the cases of its definite, free, and inertial rotation was simulated by the boundary conditions [9] for the Navier–Stokes equations in the stream function ψ–vorticity ω variables.

Formulation of the Problem. An unbounded fluid flow will be simulated by a rectangular region $D = [-L_1, L_2] \times [-H/2, H/2]$, where L_1, L_2, and $H >> 1$. A cylinder of unit radius with a boundary γ is placed at the center of the computational region $x, y = 0$. The following constitutive equations are used:

$$\frac{\partial \omega}{\partial t} + u\frac{\partial \omega}{\partial x} + v\frac{\partial \omega}{\partial y} = \frac{1}{\mathrm{Re}}\Delta\omega\,; \tag{1}$$

$$\Delta\psi = -\omega\,, \quad \omega = \frac{\partial v}{\partial x} - \frac{\partial u}{\partial y}\,, \quad u = \frac{\partial \psi}{\partial y}\,, \quad v = -\frac{\partial \psi}{\partial x}\,; \tag{2}$$

$$\Delta p = -2\left(\frac{\partial v}{\partial x}\frac{\partial u}{\partial y} - \frac{\partial u}{\partial x}\frac{\partial v}{\partial y}\right) = 2\left[\frac{\partial^2 \psi}{\partial x^2}\frac{\partial^2 \psi}{\partial y^2} - \left(\frac{\partial^2 \psi}{\partial x \partial y}\right)^2\right]. \tag{3}$$

The conditions of ideal slipping, $\psi = y$, $\omega = 0$, $\partial p/\partial n = 0$, are set at the horizontal boundaries $y = \pm H/2$; it is assumed that at the inlet $x = -L_1$ the flow is uniform, $\psi = y$, $\omega = 0$, and $p = 0$, and has a unit velocity, and the "soft" boundary conditions $\partial\psi/\partial n = 0$, $\partial\omega/\partial n = 0$, $\partial p/\partial n = 0$ are set at the output cross section $x = L_2$. The following boundary conditions are set at the impenetrable surface of the cylinder:

Institute of Mechanics and Mechanical Engineering, Kazan' National Center of the Russian Academy of Sciences, 2/31 Lobachevskii Str., Kazan', 420111, Russia; email: amazo@ksu.ru. Translated from Inzhenerno-Fizicheskii Zhurnal, Vol. 79, No. 3, pp. 75–81, May–June, 2006. Original article submitted November 2, 2004.

1062-0125/06/7903-0496

$$x, y \in \gamma: \quad \psi = \psi_0, \quad \frac{\partial \psi}{\partial n} = v_0, \quad \frac{\partial p}{\partial n} = \frac{1}{\mathrm{Re}} \frac{\partial \omega}{\partial s}. \tag{4}$$

As was shown in [9], the constant ψ_0 is expressed at each instant of time t in terms of the vorticity ω and the auxiliary function $\eta(x, y)$:

$$\psi_0 = \frac{1}{|\gamma|} \int_D \omega (\eta - \bar{\eta})\, dD, \quad \bar{\eta} \equiv \frac{1}{|\gamma|} \int_\gamma \eta ds, \tag{5}$$

where $|\gamma| = 2\pi$ is the length of the boundary and η is a solution of the boundary problem

$$\Delta \eta = 0, \quad x, y \in D; \quad x = -L_1, L_2: \frac{\partial \eta}{\partial n} = 0; \quad y = \pm H/2: \eta = 0; \quad \gamma: \frac{\partial \eta}{\partial n} = 1. \tag{6}$$

In the problem considered, the tangential velocity $v_0(t)$ determines the angular rotational velocity of the cylinder; therefore, the case where the cylinder remains in position ($v_0 = 0$) and the case where it executes a regular rotation ($v_0 = \mathrm{const}$) are described by relations (4) and (5). However, in problems on the interaction of a viscous flow with a cylinder having a rotational degree of freedom it is necessary to additionally determine the velocity v_0. In the case of free rotation of the cylinder (weightless cylinder), the equation for this velocity expresses the absence of a summary shear stress σ_0/Re on the cylinder surface and has the form

$$\sigma_0 (v_0) = \int_\gamma \omega ds = 0. \tag{7}$$

If the cylinder has an inertia, $\sigma_0(t)$ is determined by solving the problem [9]

$$\frac{dv_0}{dt} = -\frac{2}{\pi\, \mathrm{Re}\, K_\rho} \sigma_0 (v_0), \quad v_0 (0) = 0, \quad K_\rho = \frac{\rho_c}{\rho}. \tag{8}$$

As $K_\rho \to 0$, Eq. (8) is rearranged to give condition (7).

The behavior of the functions $\psi_0(t)$, $\sigma_0(t)$, and $v_0(t)$ is of interest not only for determining the dynamics of the drag coefficient, lifting force

$$C_x = \int_\gamma \frac{\omega \cos (\widehat{\tau, x})}{\mathrm{Re}} + p \sin (\widehat{s, x})\, ds, \quad C_\gamma = \int_\gamma \frac{\omega \sin (\widehat{\tau, x})}{\mathrm{Re}} + p \cos (\widehat{\tau, x})\, ds \tag{9}$$

and the Strouhal number $\mathrm{Sh} = 2f$, but also for stimulation of nonstationary flows around a rotating cylinder. The pressure p is determined from the Poisson equation (3) with the right side expressed in terms of the second derivatives of the stream function ψ. Methods of numerically solving the Navier–Stokes equations (1)–(3) with boundary conditions (4)–(6) and additional equations (8) and (9) as well as an algorithm for calculating the pressure are presented in [4, 9]. The basic equations (1) and (2) were solved by the first-order finite-element method (linear basis functions), and the pressure p was calculated using the second- and third-order triangular elements.

In the present work, an alternative approach was used for calculating the pressure [10]. According to this approach, the boundary problem for the Bernoulli variable $B = p + V^2/2$, $\mathbf{V} = (u, v)$ is solved instead of problem (3), (4):

$$-\Delta B = \mathrm{grad}\, \omega \cdot \mathrm{grad}\, \psi - \omega^2; \quad \gamma: \frac{\partial B}{\partial n} = \frac{1}{\mathrm{Re}} \frac{\partial \omega}{\partial s} - v_\tau \omega. \tag{10}$$

In problem (10), to calculate the right sides of the equations it will suffice to take the first derivatives of the difference values of ψ and ω; therefore, B can be calculated using the linear finite elements of the main problem (1), (2).

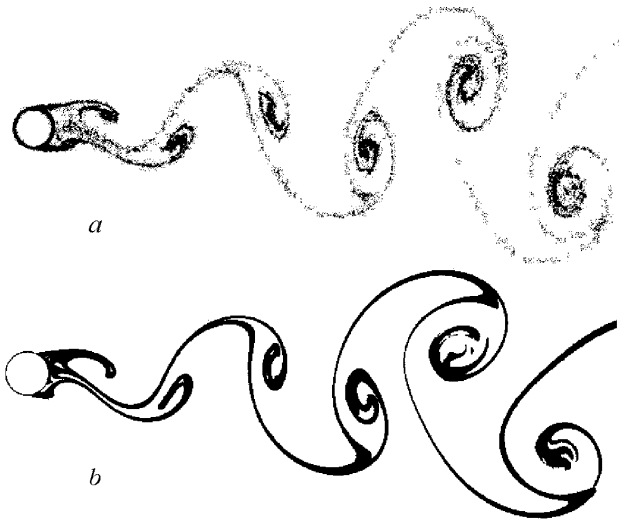

Fig. 1. Kármán vortex street downstream of a circular cylinder at Re = 105: a) calculation result; b) experimental photography [11].

Below are results of a computational experiment.

In the calculations, the region D was defined by the parameters $H = 60$, $L_1 = 25$, and $L_2 = 200$, which provided a negligibly small influence of the outer boundaries on the numerical solution of the problem. An irregular triangular finite-element grid with a significant bunching of nodes in the neighborhood of the cylinder was used; the total number of nodes and elements was, respectively, 9924 and 19,639 and the ratio between the areas of the maximum and minimum elements of the grid was of the order of 6500. The mean time of calculating the functions ψ and ω for the transient period $t \sim 150$ sec with a step of 0.025 on an Athlon-1700 computer was 20 min. To calculate the pressure on the basis of this grid, a grid of six-node square elements with 38,487 nodes was constructed; the time of calculation was about 20 sec per time step.

Results of Numerical Simulation. *Immovable cylinder.* A laminar flow around an individual immovable cylinder has been much studied (see, e.g., [1–3]) and is of interest mainly for testing a numerical algorithm. We performed test calculations of the indicated flow earlier at small and moderate Re numbers, where a stationary solution of the problem exists; the results of these calculations are presented in [4]. The results of simulation performed for $41 < \mathrm{Re} < 160$, at which a two-dimensional stream flows around a cylinder in the self-oscillation regime [1, 3], were compared with the data of other authors and experimental data on the general pattern of flow, the dependence of the rate of vortex formation on the Reynolds number, and the average coefficients C_x and C_y and amplitudes of their oscillations at different Re.

For visualization of a flow, we simulated an outflow of smoke (weightless marked particles) from the surface of a cylinder and its propagation in the wake downstream of the cylinder, as is done in natural experiments. The calculation results compared with experimental photography [11] are shown in Fig. 1.

The development of self-oscillations is conveniently illustrated by the graphs of the functions $\psi_0(t)$ and $\sigma_0(t)$. Figure 2 shows the dependences $\psi_0(t)$ determined by formula (5) for Re = 70 and 150. It is seen that, with increase in the Reynolds number, the symmetric pattern of flow breaks down, a periodic regime is established earlier, and the amplitude of the self-oscillations increases.

The rate of vortex formation is also conveniently determined by these graphs. The dependence Sh(Re) obtained was practically coincident with the calculation prediction done in [2] and agreed wholly satisfactorily with the numerical and experimental results of other authors [3, 6]. In the range of Reynolds numbers considered, this dependence can be approximated to sufficient accuracy by the formula [5]

$$\mathrm{Sh} = 0.266 + (-1.02/\sqrt{\mathrm{Re}}), \quad 41 < \mathrm{Re} < 160 .$$

The drag and lift coefficients (9) also experience harmonic oscillations in the process of periodic separation of vortices; in this case, the frequency of oscillations of C_y is equal to the frequency of oscillations of the function Sh(t)

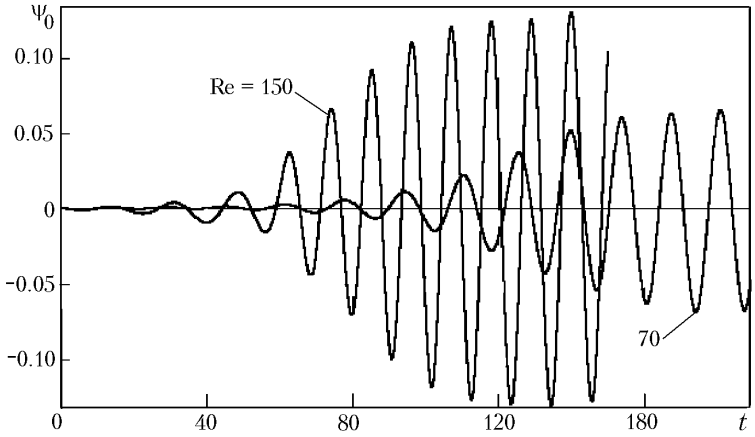

Fig. 2. Self-oscillations of the boundary value of the stream function $\psi_0(t)$ at Re = 70 and 150.

TABLE 1. Dependence of the Drag Coefficient and the Amplitudes of Oscillations of the Drag and Lift Coefficients on the Reynolds Number

Re	70	100	150
$\overline{C}_x$	1.367	1.337	1.331
A_x	0.004	0.010	0.019
A_y	0.146	0.259	0.409

TABLE 2. Influence of the Rotational Velocity on the Drag and Lift Coefficients at Re = 100

v_0	0	0.5	1.0	1.5
$\overline{C}_x$	1.34	1.28	1.11	0.82
$\overline{C}_y$	0.00	1.22	2.50	3.90

and the frequency of oscillations of C_x is two times higher. The drag coefficient $\overline{C}_x$ averaged over the oscillation period, the amplitude of its change A_x, and the amplitude of oscillations of the lift coefficient A_y are dependent on the Reynolds number (Table 1). It was established that the average drag coefficient $\overline{C}_x$ decreases and the amplitudes A_x and A_y increase with increase in Re. The calculated values of the drag and lift coefficients agree fairly well with the data of [2, 3, 5].

Definite rotation. The pattern of a flow around a cylinder rotating with a constant velocity differs qualitatively from the pattern of a flow around an immovable cylinder. In the case of rotation in a counterclockwise direction, the vortex wake shifts up relative to the line $y = 0$ (see Fig. 3). The width of the vortex wake decreases with increase in v_0.

The influence of the rotational velocity on the process of periodic separation of vortices was investigated in [6–8]. According to the data of [8], Sh decreases with increase in v_0, while the opposite result was obtained in [6]. According to our calculations, the Strouhal number increases insignificantly with increase in v_0 (by no more than 1% when v_0 changes from 0 to 2).

In [6–8], the influence of the rotational velocity on the suppression of the periodic separation of vortices was investigated. The authors of these works argued that, to each value of Re corresponds a critical rotational velocity v_0^* such that, at $v_0 < v_0^*$, self-oscillations arise, and, at $v_0 > v_0^*$, a stationary flow regime is established. In [8], this phenomenon was called the bifurcation of a flow around a rotating cylinder. Our calculations have shown that, in actuality, self-oscillations are suppressed at certain rotational velocities, which manifests itself as a gradual decrease in the amplitude of self-oscillations of the functions $\psi_0(t)$ and $\sigma_0(t)$ with increase in v_0 at a constant value of Re. Figure 4 shows the dependence of the amplitude of self-oscillations of the shear stress on the rotational velocity of the cylinder at Re = 160. It is seen that the suppression of vortices begins at $v_0^* = 1.6$ and the self-oscillations terminate at $v_0^* =$

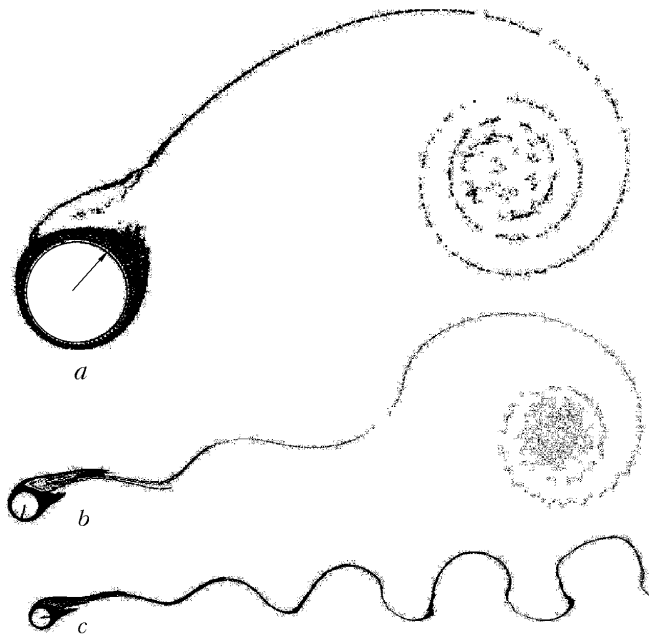

Fig. 3. Development of a flow near a rotating cylinder at v_0 = 2.0 and Re = 100: t = 12.5 (a), 42.5 (b), and 100 (c).

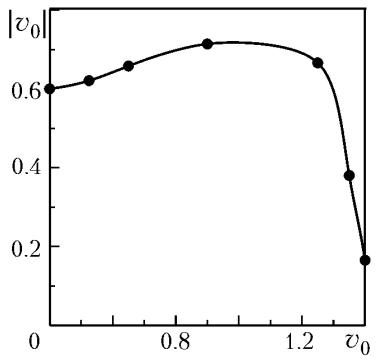

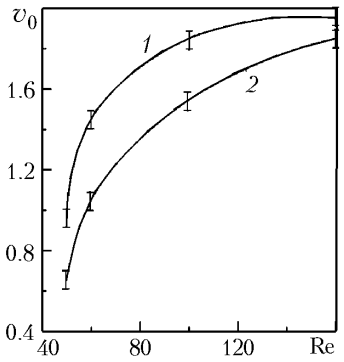

Fig. 4. Dependence of the amplitude of self-oscillations of the shear stress on the rotational velocity of a cylinder.

Fig. 5. Dependence of the critical rotational velocity of a cylinder on the Reynolds number.

2. For other Reynolds numbers, the corresponding intervals are shown in Fig. 5 (curve 2) in comparison with the analogous data obtained in [6] (curve 1).

It is known [5] that the rotational velocity of a cylinder substantially influences its drag and lift coefficients averaged over the self-oscillation period. The results of our calculations (some of them are presented in Table 2) point to the existence of this influence. They indicate that C_x somewhat decreases and C_y markedly increases with increase in the rotational velocity of the cylinder v_0.

Free and inertial rotation. If a cylinder rests on a fixed axis and has a rotational degree of freedom, a periodic separation of vortices from its surface gives rise to self-oscillations of the cylinder itself. The frequency and amplitude of oscillations of the angular velocity v_0 increase with increase in Re.

The dependence Sh(Re) for a freely rotating weightless cylinder (boundary condition (7)) differs by no more than 1.5% from the analogous dependence for an immovable cylinder and the hydrodynamical drag decreases, on average, by 10%.

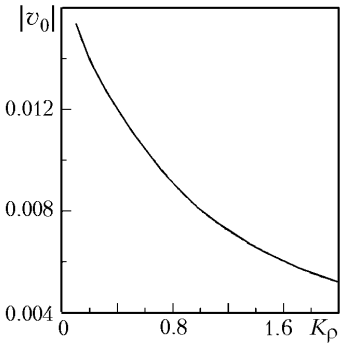

Fig. 6. Influence of the inertia on the amplitude of self-oscillations of the rotational velocity of a cylinder.

The interaction of a flow with a cylinder possessing an inertia (boundary condition (8)) is qualitatively identical to that in the above-indicated case. The criterion K_ρ practically does not influence the frequency of the forced oscillations; however, the amplitude of oscillations of the rotational velocity $|v_0(t)|$ decreases with increase in K_ρ, as is shown in Fig. 6.

CONCLUSIONS

1. A nonstationary flow around a cylinder having a rotational degree of freedom has been numerically investigated on the basis of the Navier–Stokes model in the stream function–vortex–pressure variables. The range of Reynolds numbers at which a self-oscillation regime of flows around the cylinder being considered is realized, has been considered.

2. For a forced rotation of a cylinder with a constant velocity, the dependence of the Strouhal number on the Reynolds number has been calculated. It has been shown that the rotational velocity practically has no influence on the frequency of the self-oscillations but decreases the amplitude of oscillations of the shear stress, somewhat decreases the drag, and leads to the appearance of a lift.

3. The interaction of a viscous flow with a weightless cylinder or a massive cylinder having a rotational degree of freedom leads to the appearance of self-oscillations of the cylinder itself. The mass of the cylinder practically has no influence on the rate of vortex formation but decreases the amplitude of oscillations of the rotational velocity.

This work was carried out with financial support from the Russian Basic Research Foundation (grants 03-01-00015, 03-01-96237) and the program "Universities of Russia" (grant 04.01.009).

NOTATION

A_x and A_y, amplitudes of oscillations of the drag and lift coefficients; C_x and C_y, drag and lift coefficients; D, computational region; H, width of a channel; L_1 and L_2, coordinates of the input and output boundaries; ds, element of an arc of the profile γ; f, rate of vortex formation; K_ρ, dimensionless density criterion; n, outer normal to the boundary; p, pressure; Re, Reynolds number; Sh, Strouhal number; t, time; $\mathbf{V}$, velocity vector; $v_0(t)$, angular rotational velocity of a cylinder; x, y, Cartesian coordinates; γ, boundary of a cylinder; ρ, density of a fluid, kg/m^3; ρ_c, density of the material of a cylinder, kg/m^3; τ, tangent; σ_0, shear stress; η, auxiliary function; ψ, stream function; ω, vorticity. Subscripts: c, cylinder.

REFERENCES

1. C. H. K. Williamson, Vortex dynamics in the cylinder wake, *Annual Rev. Fluid. Mech.*, No. 28, 477–539 (1996).
2. A. V. Ermishin and S. A. Isaev (Eds.), *Control of Flows Past Bodies with Vortex Cells as Applied to Flying Vehicles of Integral Arrangement* (*Numerical and Physical Simulation*) [in Russian], Izd. MGU, Moscow (2003).

3. O. Posdziech and R. Grundmann, Numerical simulation of the flow around an infinitely long circular cylinder in the transition regime, *Theor. Comput. Fluid Dyn.*, No. 15, 121–141 (2001).
4. A. B. Mazo and I. V. Morenko, Drag and rotational properties of cascades of circular cylinders at small and moderate Reynolds numbers, *Inzh.-Fiz. Zh.*, **77**, No. 2, 75–79 (2004).
5. D. Stojković, M. Breuer, and F. Durst, Effect of high rotation rates on the laminar flow around a circular cylinder, *Phys. Fluids*, **14**, No. 9, 3160–3178 (2002).
6. S. Kang, H. Choi, and S. Lee, Laminar flow past a circular cylinder, *Phys. Fluids*, **11**, No. 11, 3312–3321 (2002).
7. F. J. Barnes, Vortex shedding in the wake of a rotating circular cylinder at low Reynolds numbers, *J. Phys. D: Appl. Phys.*, No. 33, L141–L144 (2000).
8. G-H. Hu, D-J. Sun, X-Y. Yin, and B-G. Tong, Hopf bifurcation in wake behind a rotating and translating circular cylinder, *Phys. Fluids*, **8**, No. 7, 1972–1974 (1996).
9. A. B. Mazo and R. Z. Dautov, On the boundary conditions for Navier–Stokes equations in stream function–vorticity variables in simulation of a flow around a system of bodies, *Inzh.-Fiz. Zh.*, **78**, No. 4, 136–142 (2005).
10. C. A. J. Fletcher, *Computational Techniques for Fluid Dynamics* [Russian translation], Vol. 2, Mir, Moscow (1991).
11. M. Van Dyke, *An Album of Fluid Motion* [Russian translation], Mir, Moscow (1986).